A gravity-driven electric current in the Earth's ionosphere identified in CHAMP satellite magnetic measurements

S. Maus

Cooperative Institute for Research in Environmental Sciences, University of Colorado, Boulder, Colorado, USA

National Geophysical Data Center, NOAA, Boulder, Colorado, USA

H. Lühr

GeoForschungsZentrum, Potsdam, Germany

Received 19 August 2005; revised 20 October 2005; accepted 14 November 2005; published 28 January 2006.

[1] A gravity field acting on a collisionless, magnetized space plasma causes electrons and ions to drift into opposite directions, in addition to gyrating around the magnetic field lines. This sets up an electric current which flows perpendicular to the gravity and magnetic fields in the eastward direction. Here we present the first observational evidence for such a gravity-driven current system in the Earth's low-latitude ionosphere. Its magnetic field signal, although 10,000 times smaller than the ambient Earth's magnetic field, is clearly visible in CHAMP satellite magnetic measurements. We find a current ribbon of more than 50 kA, about 66° wide in latitude, which moves with the sun northward in summer and southward in winter. Correcting magnetic measurements for this current's signature should lead to a better agreement between low-orbiting satellite and ground-based observations. **Citation:** Maus, S., and H. Lühr (2006), A gravity-driven electric current in the Earth's ionosphere identified in CHAMP satellite magnetic measurements, *Geophys. Res. Lett.*, *33*, L02812, doi:10.1029/2005GL024436.

1. Introduction

[2] Extreme ultraviolet (EUV) radiation from the Sun ionizes the neutral gas of the Earth's atmosphere, generating the ionosphere. With regard to electric currents, the ionosphere can be divided primarily into two layers, the E region at about 90 to 150 km altitude, and the F region above it [*Volland*, 1985; *Parks*, 2004].

[3] In the E region, the density of neutral particles is by several orders of magnitude higher than the density of ions, preventing ions (but not electrons) from gyrating around the magnetic field lines. Neutral winds drag ions along with them, leading to charge separation and large scale electric fields and dynamo currents. The recombination rate at low altitudes is high, therefore the E region with its dynamo currents disappears after sun set, except at high latitudes where particle precipitation contributes significantly to the ionization. E region currents, e.g. the Sq system, are seen as daily magnetic variations in ground observatory records [*Chapman and Bartels*, 1940].

[4] The F region, with its lower neutral gas density, behaves more like a collisionless space plasma. Here the recombination rate is low, so that the F region persists throughout the night. Electric currents in the F region are generally much weaker and more difficult to detect. For example, a meridional current system at equatorial latitudes predicted by *Untiedt* [1967] and *Sugiura and Poros* [1969] was identified by *Musmann and Seiler* [1978] in sounding rocket magnetic field measurements and by *Maede et al.* [1982] in Magsat satellite data. Magsat observations also contained the signatures of inter-hemispheric field aligned currents, as reported by *Olsen* [1997]. Currents associated with local plasma depletions were first identified by *Lühr et al.* [2002] in CHAMP measurements. *Eccles* [2004] pointed out that the force of gravity should be a measurably important driver for currents in the low-latitude ionosphere. Here, we present the first observational evidence for such a gravity-driven current system.

2. Currents in the Ionospheric F Region

[5] Apart from winds, active drivers of electrical currents in the F region include ionospheric plasma pressure gradients and the Earth's gravity field. Both effects depend on the density of the F region plasma, which usually peaks at an altitude of around 300 km. The relevant contributions to the current density are [*Kelly*, 1989, section 4.2]

$$\mathbf{j} = \underline{\underline{\sigma}}\mathbf{E} + \{n\, m_i\, \mathbf{g} \times \mathbf{B} - k\, \nabla[(T_i + T_e)\, n] \times \mathbf{B}\}\, \frac{1}{B^2} \qquad (1)$$

where $\underline{\underline{\sigma}}$ is the conductivity tensor, $\mathbf{E}$ is the electric field, n the electron density, m_i the ion mass, $\mathbf{g}$ is the gravitational acceleration, k is the Boltzmann constant, T_e and T_i are the electron and ion temperatures, and $\mathbf{B}$ is the ambient magnetic field with its magnitude B. At night time the first term on the right-hand side represents primarily Pedersen currents, the second gravity-driven currents and the third term the currents driven by the pressure gradient. It is readily seen that the gravity force can have a significant effect only at lower latitudes where the magnetic field is predominantly horizontal.

[6] In the following, we use the term "primary currents" for the local gravity and pressure drivers of the currents. To find the "true currents" one has to take the large-scale secondary electric fields and the conductivity structure of the ionosphere into account, corresponding to the first term in equation (1). The primary current density $\mathbf{j} = \mathbf{j}_{\nabla p} + \mathbf{j}_g$ can be separated into a non-divergent (source-free) and a divergent (irrotational) part. The non-divergent part can be

0094-8276/06/2005GL024436$05.00

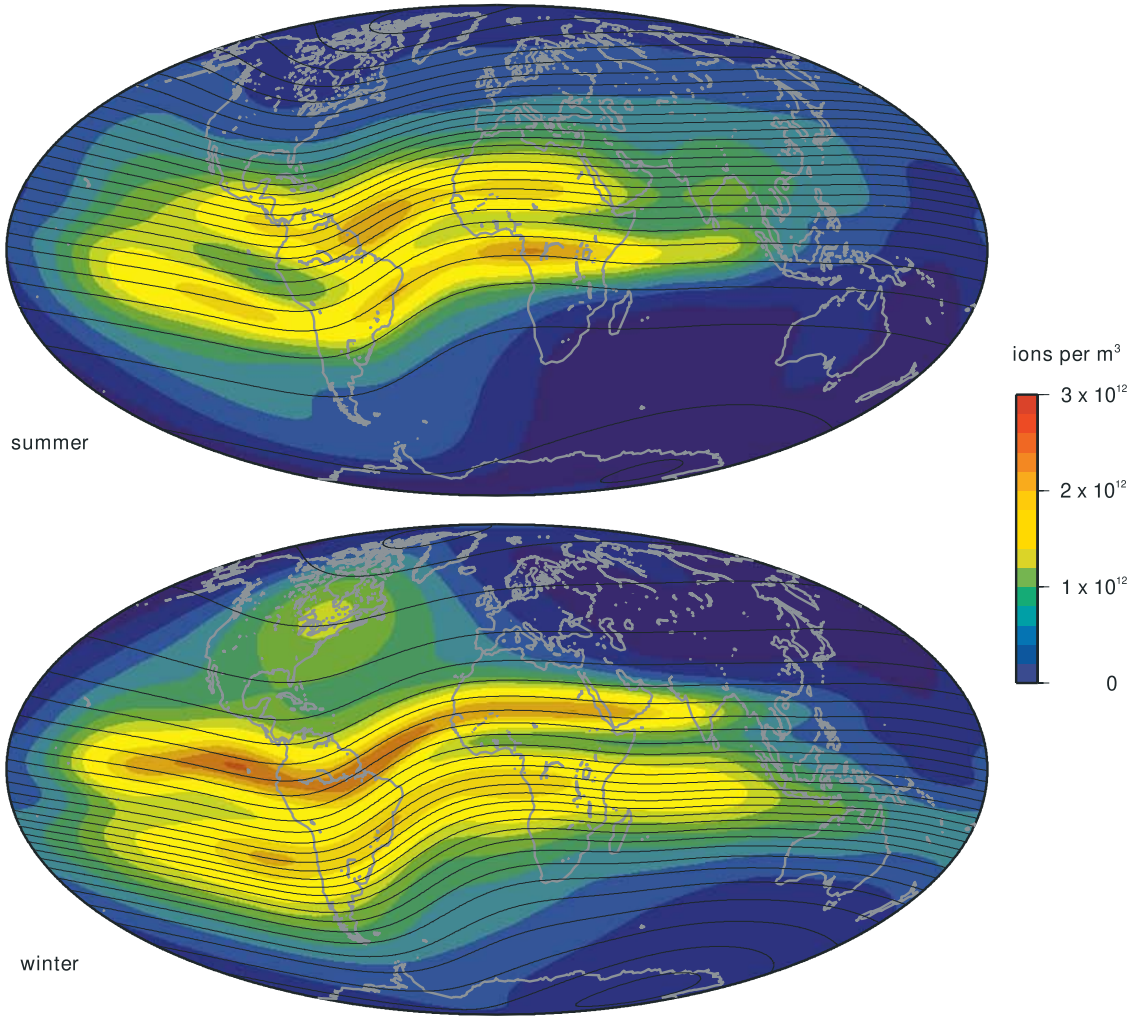

Figure 1. Ion density from the International Reference Ionosphere (IRI) displayed as color maps for a summer (21 June 2000) and a winter day (20 December 2000) for an altitude of 400 km at 18:00 UT. Overlain are the current lines of the non-divergent part of the primary gravity-driven current. A sheet current with a density of 1 mA/m flows eastward between any two neighboring isolines of the stream function.

thought of as the free-flowing, unrestricted part of the current. In contrast, the divergent part builds up a large-scale charge distribution which is the source of a secondary electric field. The total electric field, which also contains contributions from the wind driven dynamo, partly inhibiting the divergent part of the primary current, is also the source of secondary currents. These effects of the electric field are represented by the first term in equation (1). Solving for these induced and wind-driven electric fields and their secondary currents is challenging since it requires solving a 3D induction problem for the entire ionosphere.

3. Model

[7] For a first order model prediction of magnetic signals of pressure gradient and gravity-driven currents in the F region we adopt the following simplifying assumptions:

[8] 1. We assume that the magnetic pressure balances the plasma pressure, neglecting inertial effects and the curvature of the geomagnetic field. As shown by *Lühr et al.* [2003], the magnetic signature of the pressure driven current can then be expressed as a scalar diamagnetic effect, b,

$$b = \frac{nk\mu_0}{B}(T_i + T_e), \tag{2}$$

which only depends on the local plasma density, ion and electron temperatures and the strength of the ambient magnetic field. The diamagnetic effect, b, represents the local reduction of the magnetic field strength. The corresponding change in the magnetic field vector, $\Delta\mathbf{B}_d$, is then given by

$$\Delta\mathbf{B}_d = b\frac{\mathbf{B}}{B}. \tag{3}$$

[9] 2. We assume that the divergent part of the primary gravity-driven current is completely inhibited by an induced electric field. The remaining gravity-driven current is then

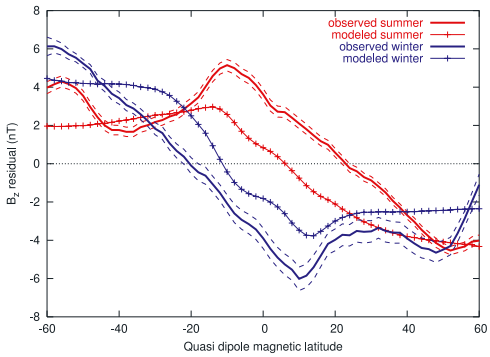

Figure 2. Mean of CHAMP vertical field residuals (positive down) at 20–22 LT, separately averaged for about 600 summer (red) and 700 winter orbits (blue). The standard deviation of the mean is indicated by dashed lines. Also shown are the corresponding predictions of our first order model, including gravity and pressure driven currents. The latter have only a small effect on the vertical magnetic field component, though.

strictly horizontal, perpendicular to the magnetic field lines, and divergence free.

[10] Assumption 1 allows us to estimate the diamagnetic field from the ambient electron density and temperature measurements of the CHAMP Planar Langmuir Probe. Typical electron temperatures are in the range of 1000 to 5000 Kelvin (K). For the ion temperatures, which are less variable, we assume a mean value of 900 K, decreasing to 800 K at 02 local time (LT) and increasing to 1000 K at 14 LT [*Köhnlein*, 1986].

[11] Utilising assumption 2 is slightly more challenging, since it requires knowledge of the ion density in the entire ionosphere. We take the densities from the International Reference Ionosphere, IRI-2000 [*Bilitza*, 2001], and determine the primary gravity-driven current, as given by the second term in (1), on 46 horizontal shells with a vertical spacing of 20 km. For each shell, we then find the non-divergent, freely flowing part of the current. In this approximation, the current density at a particular height and magnetic latitude is controlled by the longitudinal sector in which the primary gravity-driven current is lowest (the "bottleneck"). In particular, stronger primary currents on the day-side, where the plasma density is higher, are thus largely inhibited by the lower densities on the night side. Integrating over the magnetic effects of the currents in all shells, we obtain the magnetic signal at the measurement locations along the satellite orbit. Examples of our approximation of the non-divergent gravity-driven current for summer and winter are given in Figure 1, underlain by the ionospheric ion density.

4. Results

[12] The satellite CHAMP (CHallenging Microsatellite Payload, http://op.gfz-potsdam.de/champ) was launched on 15 July 2000 into a circular, near-polar orbit at 450 km altitude [*Reigber et al.*, 2002]. As of August 2005, the altitude has decayed to 360 km. The high-precision CHAMP magnetic field instrumentation is ideally suited for the present study. We use measurements of the Overhauser magnetometer for the field intensity and the Fluxgate magnetometer for the field vector covering the years 2000 through 2004. Data are selected from the 20-22 local time (LT) sector, when the F region ion density is still high and the E region currents have subsided. We use only measurements during magnetically quiet times, as indicated by values of the magnetic activity indices, $K_p \leq 2$ and $|Dst| \leq 30$. The next step is to subtract the magnetic field signatures of the major contributions from the Earth's core field, induction in the mantle, crustal magnetization, ocean tidal induction, and the magnetospheric currents. We use the model POMME-2.5 [*Maus et al.*, 2005], subtracting an internal field up to spherical harmonic degree 90, secular variation to degree 16, secular acceleration to degree 12, and magnetospheric fields to degree 2, including new parameterizations for induction effects [*Maus and Weidelt*, 2004; *Maus and Lühr*, 2005]. Ocean tidal fields are subtracted to degree 45 [*Maus and Kuvshinov*, 2004]. The resulting residuals derived from about 1300 satellite orbits are averaged over all longitudes in 2 degree bins of corrected magnetic latitude [*Richmond*, 1995]. Our first-order model predictions are computed for the same times and locations as the satellite data sampling, and are averaged in the same way as the measurements.

[13] Figure 2 displays meridional profiles of the observed magnetic residuals in the downward component, B_z, averaged separately for the summer and winter months. The comparison with our first-order model shows that the residual field is indeed explained by an eastward directed gravity-driven current. The current system is shifted northward in northern summer and southward in northern winter. There are a number of interesting features which can be deduced from the shape of the curves: The zero-crossings mark the center magnetic latitude of the current band. The observations exhibit center latitudes of ±23° for the summer

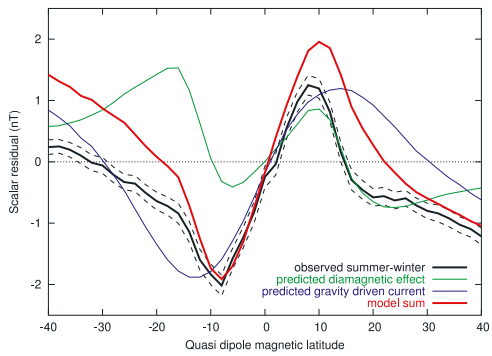

Figure 3. Observed seasonal difference (black) between the means of CHAMP magnetic field intensity residuals at 20–22 LT for the same summer and winter orbits as in Figure 2. The standard deviation of the mean of the observed seasonal difference is indicated by dashed lines. The colored curves show the corresponding predictions from our first-order model for pressure (green) and gravity (blue) driven currents. Both effects contribute significantly to the intensity of the field. The sum of both predictions (red) is in good agreement with the observed seasonal variation (black).

and winter seasons, respectively. This suggests that the F region ionization is symmetrical about the sub-solar point. The model curves, on the other hand, have zero-crossings only 10° away from the magnetic equator, predicting a smaller seasonal variation of the ionization. From the field gradient in the vicinity of the zero-crossing, the height-integrated current density can be estimated. We obtain 6.5 and 8 mA/m for the summer and winter months, respectively. The slightly higher value in winter may be due to the higher magnetic activity during that season. From our model, we predict quite similar current densities. The extrema of the vertical component are expected to be located at the northern and southern boarders of the main current ribbon around the Earth. There are clear positive and negative peaks at ±10° for the summer and winter curves. The antipodal peaks, expected at ±56° magnetic latitude, are not so well discernible in the observations, due to the vicinity to the auroral regions with their disturbing current systems. The fairly homogeneous current band thus exhibits a latitudinal width of about 66°. In contrast, our model predicts a width of only about 40° in latitude. Overall, our first-order model reproduces the main features of the magnetic signatures reasonably well, but underestimates the total F region current and its seasonal variability.

[14] So far we have concentrated on the vertical field signatures. The advantage of this component is that it depends little on the altitude difference between observation and current. Therefore, the orbital decay of CHAMP and a change in F region height have little impact on the results. The horizontal component, on the other hand, varies strongly with height. It changes sign through the current sheet and is zero at the center altitude. From this component we thus may obtain an idea of the height at which the currents flow. In attempting to identify the height-sensitive signatures in the horizontal component, one has to take into account that steady parts of this signal may have incorrectly been attributed to other contributions, like core and crustal fields. However, this unknown constant bias does not affect a comparison between seasons.

[15] To investigate seasonal variations, we use the scalar residual (the deviation in field strength is a particularly accurate measurement), instead of the horizontal vector components. At low latitudes the scalar residual is similar to the northward component. Figure 3 shows meridional profiles of the average observed and predicted seasonal variation in the scalar residuals at 20–22 LT. For the observed seasonal difference (northern summer minus northern winter) we find extrema at ±8° magnetic latitude. These latitudes agree well with the location of the equatorial ionization anomaly (EIA) at this local time. As expected for an eastward current which is raised in local summer and lowered in local winter, we find a positive seasonal difference in the northern and a negative difference in the southern hemisphere.

5. Conclusions

[16] The existence of an eastward directed, gravity-driven electric current in the Earth's ionosphere follows directly from the equation of motion for the F-region plasma, as given in equation (1) in terms of the current density. Its magnetic signature is strong enough to be observed by the low orbiting CHAMP satellite. Several distinct features of the F region plasma in the early night time sector can be deduced from our observations:

[17] 1. There is a zonal band of enhanced electron content, more than 60° wide, which follows the sub-solar latitude,

[18] 2. The height-integrated current density is about 7 mA/m at its center,

[19] 3. From this current a peak electron content in the post-sunset sector can be estimated to 80 TEC (Total Electron Content) units, assuming an O^+ ionosphere,

[20] 4. The total eastward current adds up to more than 50 kA,

[21] 5.These currents cause magnetic fields of the order of ±5 nT below and above the F region.

[22] We find a reasonable agreement of the observed magnetic signatures with the predictions from our first-order model. The model underestimates the total F region current and its seasonal variability. This is likely to be partly due to our simplifying assumption that the divergent part of the primary gravity-driven current is completely inhibited. However, inaccuracies in the ionospheric density model used for our prediction may also play a role.

[23] Taking gravity-driven currents into consideration will have a noticeable impact on the accuracy of geomagnetic field models. Correcting for these currents will significantly reduce the noise due to unmodeled sources and lead to a better agreement between observatory and satellite magnetic measurements. It will be a key issue for joint interpretations of magnetic and ionospheric data from satellites at different altitudes, and it is of particular importance for the upcoming *Swarm* constellation mission, which includes satellites at different heights and local times. The interpretation of ionospheric magnetic signatures using more accurate current models could provide an independent validation of ionospheric density and temperature models.

[24] Similar currents must exist on other planets in the universe. As can be seen from equation (1), the current requires a dense, collisionless ionosphere and a weak intrinsic magnetic field. For the planets in our solar system, the Earth currently appears to have the most favorable conditions.

[25] **Acknowledgments.** The operational support of the CHAMP mission by the German Aerospace Center (DLR) and the financial support for the data processing by the Federal Ministry of Education and Research (BMBF) are gratefully acknowledged.

References

Bilitza, D. (2001), International Reference Ionosphere 2000, *Radio Sci.*, *36*, 261–275.

Chapman, S., and J. Bartels (1940), *Geomagnetism*, Oxford Univ. Press, New York.

Eccles, J. V. (2004), The effect of gravity and pressure in the electrodynamics of the low-latitude ionosphere, *J. Geophys. Res.*, *109*, A05304, doi:10.1029/2003JA010023.

Kelly, M. C. (1989), *The Earth's Ionosphere*, Elsevier, New York.

Köhnlein, W. A. (1986), A model of the electron and ion temperatures in the ionosphere, *Planet. Space Sci.*, *34*, 609–630.

Lühr, H., S. Maus, M. Rother, and D. Cooke (2002), First in situ observation of night time F region currents with the CHAMP satellite, *Geophys. Res. Lett.*, *29*(10), 1489, doi:10.1029/2001GL013845.

Lühr, H., M. Rother, S. Maus, W. Mai, and D. Cooke (2003), The diamagnetic effect of the equatorial Appleton anomaly: Its characteristics and impact on geomagnetic field modeling, *Geophys. Res. Lett.*, *30*(17), 1906, doi:10.1029/2003GL017407.

Maede, H., T. Iyemori, T. Araki, and T. Kamei (1982), New evidence of a meridional current system in the equatorial ionosphere, *Geophys. Res. Lett.*, *9*, 337–340.

Maus, S., and A. V. Kuvshinov (2004), Ocean tidal signals in observatory and satellite magnetic measurements, *Geophys. Res. Lett.*, *31*, L15313, doi:10.1029/2004GL020090.

Maus, S., and H. Lühr (2005), Signature of the quiet-time magnetospheric magnetic field and its electromagnetic induction in the rotating Earth, *Geophys. J. Int.*, *162*, doi:10.1111/j.1365-246X.2005.02691.x.

Maus, S., and P. Weidelt (2004), Separating the magnetospheric disturbance magnetic field into external and transient internal contributions using a 1D conductivity model of the Earth, *Geophys. Res. Lett.*, *31*, L12614, doi:10.1029/2004GL020232.

Maus, S., H. Lühr, G. Balasis, M. Rother, and M. Mandea (2005), Introducing POMME, Potsdam Magnetic Model of the Earth, in *Earth Observation With CHAMP: Results From Three Years in Orbit*, edited by C. Reigber et al., pp. 293–298, Springer, New York.

Musmann, G., and E. Seiler (1978), Detection of meridional currents in the equatorial ionosphere, *J. Geophys. Res.*, *44*, 357–372.

Olsen, N. (1997), Ionospheric F region currents at middle and low latitudes estimated from Magsat data, *J. Geophys. Res.*, *102*, 4563–4576.

Parks, G. K. (2004), *Physics of Space Plasmas*, 2nd ed., Westwiew, Boulder, Colo.

Reigber, C., H. Luehr, and P. Schwintzer (2002), CHAMP mission status, *Adv. Space Res.*, *30*, 129–134.

Richmond, A. D. (1995), Ionospheric electrodynamics using magnetic apex coordinates, *J. Geomagn. Geoelectr.*, *47*, 191–212.

Sugiura, M., and D. J. Poros (1969), An improved model equatorial electrojet with a meridional current system, *J. Geophys. Res.*, *74*, 4025–4034.

Untiedt, J. (1967), A model of the equatorial electrojet involving meridional currents, *J. Geophys. Res.*, *72*, 5799–5810.

Volland, H. (1985), *Atmospheric Electrodynamics*, *Phys. Chem. Space*, vol. 11, Springer, New York.

H. Lühr, GeoForschungsZentrum, Telegrafenberg, D-14473 Potsdam, Germany. (hluehr@gfz-potsdam.de)

S. Maus, National Geophysical Data Center, NOAA E/GC1, 325 Broadway, Boulder, CO 80305–3328, USA. (stefan.maus@noaa.gov)